ORGANOMETALLICS

pubs.acs.org/Organometallics

Article

Synthesis, Structures, and Electronic Properties of O- and S-Heterocyclic Carbene Complexes of Iridium, Copper, Silver, and Gold

Maximilian Joost, Martin Nieger, Martin Lutz, Andreas W. Ehlers, J. Chris Slootweg, and Koop Lammertsma*

Cite This: *Organometallics* 2020, 39, 1762–1771

Read Online

ACCESS | Metrics & More | Article Recommendations | Supporting Information

ABSTRACT: O- and S-heterocyclic carbenes (OHCs, SHCs) are shown experimentally and computationally to be stronger π acceptors than NHCs and lack, of course, substituents at the heteroatoms. These different electronic and steric characteristics make OHCs and SHCs interesting ligands for coordination chemistry. Convenient synthetic routes are presented to access their iridium(I), iridium(III), and coinage-metal(I) (Cu, Ag, Au) complexes in good yields by means of dissociation of olefins, deprotonation of precursor salts, and transmetalation from a silver carbene complex. Molecular structures and detailed bonding analyses of these complexes are presented.

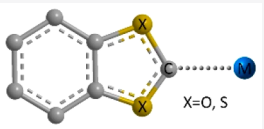

N-heterocyclic carbenes (NHCs, **I**, Figure 1)[1] have had a profound impact on organic synthesis,[2] catalysis,[3] and materials research.[4] The strong σ-donor and π-acceptor properties of the NHCs underlie the stability of their transition-metal (TM) complexes.[5] These Fischer-type carbene complexes have been heavily explored for catalysis by electronic and steric tuning of the ligands,[6] such as modifying the backbone to cyclic diamidocarbenes (**VII**), which are strongly π back-bonding, but also by replacing an NR for a CR_2 unit as in cyclic alkylaminocarbenes (CAACs, **II**)[7] and cyclic aminoarylcarbenes (CAArCs).[8] Whereas replacing NR units for oxygen or sulfur atoms should likewise have a substantial effect, it is surprising that the NOHCs (**III**)[9] and NSHCs (**IV**)[10] have been explored far more modestly.[11]

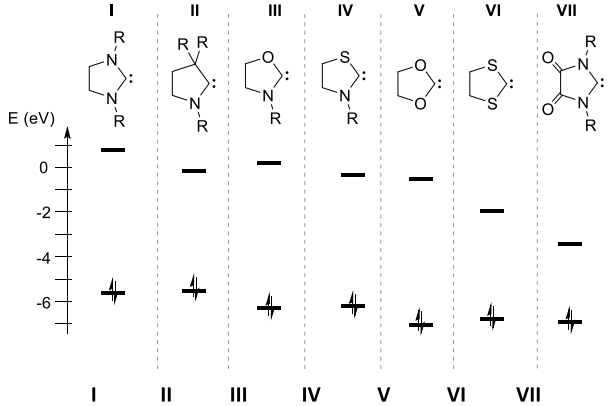

	I	II	III	IV	V	VI	VII
εLUMO	0.73	0.03	0.41	-0.18	0.30	-1.74	-3.25
εHOMO	-5.63	-5.35	-6.08	-6.04	-6.84	-6.60	-6.79
ΔE^{ST}	72.2	49.1	71.4	59.6	69.7	43.3	34.8
ΔG^{dimer}	-4.4	-35.8	-17.9	-28.0	-26.7	-55.6	-37.2

Figure 1. HOMO and LUMO energies (in eV, also visualized), singlet–triplet energy gaps (ΔE^{ST} in kcal mol^{-1}), and Gibbs free energies of dimerization (in kcal mol^{-1}) for carbenes **I**–**VII** with R = Me at the B3LYP/TZVP level.

This study focuses on O- and S-heterocyclic carbenes (OHCs (**V**) and SHCs (**VI**)) in which *both* NR units of the NHC are exchanged for O or S atoms. The coordination of these carbenes is, a priori, determined by electronic stabilization only, which is in contrast with any of the NHCs (**I**–**IV**), where the fanlike behavior of the N substituents contributes to steric shielding of the transition metal.[6a]

The electronic donor/acceptor properties of the OHC and SHC carbenes can be inferred from the relative energies of the frontier orbitals, which are compared in Figure 1 with those of the more familiar NHCs (**I**) and CAACs (**II**) as well as the NOHCs (**III**) and NSHCs (**IV**) and the cyclic diamidocarbenes (**VII**) at the B3LYP/TZVP level (R = Me) (see the Supporting Information for details).

The low energies of the carbene-centered HOMOs suggest OHCs and SHCs to be the weakest σ-donating ligands of the set, only similar to diamidocarbene **VII**. The π-acceptor ability of the carbenes increases from left to right in Figure 1 as the carbene-centered LUMO decreases in energy. The singlet–triplet energy difference (ΔE^{ST}), which is a measure for the

Received: January 30, 2020
Published: May 8, 2020

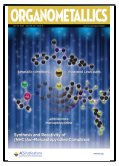

https://dx.doi.org/10.1021/acs.organomet.0c00066
Organometallics 2020, 39, 1762–1771

stability of a carbene, is a significant 69.7 kcal mol^{-1} for OHC and similar in magnitude to that of NHC **I**, while the smaller value for SHCs (43.3 kcal mol^{-1}) resembles that of diamidocarbene **VII**. The large difference in dimerization energies (ΔG^{dimer}) of OHCs (−26.7 kcal mol^{-1}) and SHCs (−55.6 kcal mol^{-1}) also suggests a higher stability for OHCa, as values of over −50 kcal mol^{-1} are indicative of reactive carbenes.[12] The calculations imply that OHCs and SHCs complement the range of available heterocyclic carbene ligands.

A number of OHC[13] and SHC complexes[13i,l,14] have been reported in the literature. To enhance their general accessibility and possibly boost their applicability, we present here three synthetic routes, akin to those developed for NHCs, to access OHC and SHC TM complexes, report on their molecular structures, and quantify their electronic characteristics.

We decided to compare the benzannulated derivatives of OHC ($\mathbf{1^O}$) and SHC ($\mathbf{1^S}$) to the NMe-substituted NHC ($\mathbf{1^N}$) (Figure 2). Their π-acceptor abilities can be estimated with the

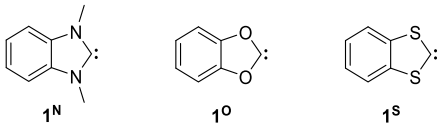

Figure 2. Benzannulated NHC, OHC, and SHC heterocyclic carbenes **1** with their respective superscript notations N, O, and S.

help of selenium adducts (Scheme 1), the electronic properties of which correlate with the ^{77}Se NMR chemical shifts; the more deshielded species correspond to the more strongly accepting carbenes.[15]

Scheme 1. Synthesis of Selones $\mathbf{1^N}$-Se, $\mathbf{1^O}$-Se, and $\mathbf{1^S}$-Se with ^{77}Se NMR Shifts

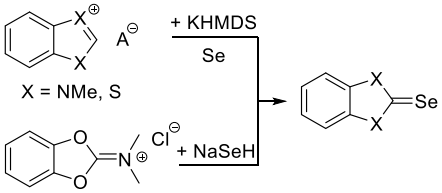

	X	δ(^{77}Se)
$\mathbf{1^N}$-Se	NMe	80
$\mathbf{1^O}$-Se	O	317
$\mathbf{1^S}$-Se	S	1017

The synthesis of the selones of $\mathbf{1^N}$, $\mathbf{1^O}$, and $\mathbf{1^S}$ is shown in Scheme 1 together with the observed ^{77}Se NMR chemical shifts. These follow the order $\mathbf{1^N}$-Se < $\mathbf{1^O}$-Se < $\mathbf{1^S}$-Se in accord with their calculated LUMO energies (see the Supporting Information). The chemical shifts for $\mathbf{1^N}$-Se (80 ppm) and $\mathbf{1^O}$-Se (317 ppm) are well within the −20 to 800 ppm range for known carbene−Se adducts and reflect OHC to be the stronger π acceptor. To the best of our knowledge, $\mathbf{1^S}$-Se has the most deshielded shift of 1017 ppm (!), suggesting this carbene to be by far the strongest π acceptor.

Carbene TM complexes are commonly generated by dissociating an alkene, deprotonating a precursor salt, or transmetalating a carbene from a silver complex.[16] For OHCs the instability of the dioxolium salts adversely affects the deprotonation route and the access to Ag complexes. Therefore, the splitting of an olefin was chosen as the starting point for the Ir complexes.

Ir COMPLEXES

Treating a solution of dibenzotetraoxofulvalene (DBTOF)[17] in toluene with $[IrCl_2(cod)]_2$ (cod = 1,5-cyclooctadiene) for 4 days at room temperature gave the red Ir(I) OHC complex $\mathbf{2^O}$ in 58% yield (Scheme 2), but SHC complex $\mathbf{2^S}$ could not be

Scheme 2. Synthesis of the Ir(I) Complex $\mathbf{2^O}$

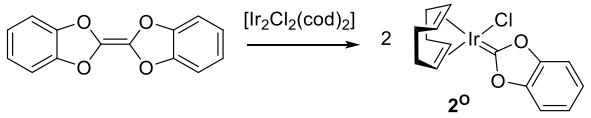

obtained in this manner from dibenzotetrathiofulvalene (DBTTF) likely due to its larger dimerization energy;[18] $[IrCl(cod)\mathbf{1^N}]$ ($\mathbf{2^N}$) was prepared via an established procedure[19] (93%; see the Supporting Information). The ^{13}C NMR spectra show a more deshielded carbene carbon for $\mathbf{2^O}$ (δ 209.2 ppm) than for $\mathbf{2^N}$ (δ 192.0 ppm), in accordance with the stronger π-accepting ability of the OHC ligand.[20] The molecular structures, determined by single-crystal X-ray structure determinations, confirmed the formation of the Ir(Cl)(cod) OHC complex $\mathbf{2^O}$ and its NHC analogue $\mathbf{2^N}$ (Figure 3). The observed Ir−carbene bond distance of

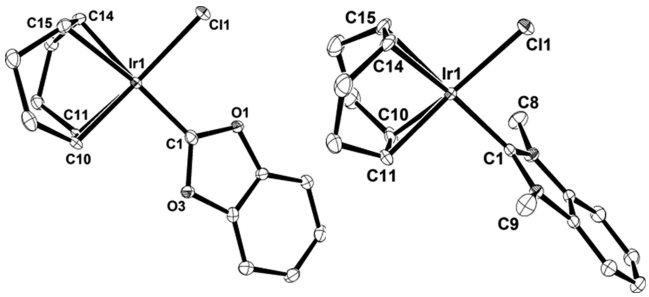

Figure 3. Structures of $\mathbf{2^O}$ (left) and $\mathbf{2^N}$ (right) in the crystal form. Ellipsoids are set at 50% probability; H atoms and solvent molecules are omitted for clarity. Selected bond lengths (Å) and angles (deg): $\mathbf{2^O}$, Ir1−C2 1.940(3), Ir1−C10 2.112(3), Ir1−C11 2.131(2), C14−C15 1.379(4), C10−C11, 1.426(4), Ir1−C14 2.226(3), Ir1−C15 2.276(3), Ir1−Cl1 2.3531(6), O1−C2 1.349(3), C2−O3 1.346(3), C2−Ir1−Cl1 91.67(7), O3−C2−O1 108.7(2); $\mathbf{2^N}$, Ir1−C1 2.0226(19), Ir1−C10 2.106(2), Ir1−C11 2.1120(19), C14−C15 1.383(3), C10−C11, 1.413(3), Ir1−C14 2.1860(19), Ir1−C15 2.2061(19), Ir1−Cl1 2.3585(5), N1−C1 1.359(2), C1−N2 1.357(2), C1−Ir1−Cl1 88.76(5), N1−C1−N2105.66 (16).

1.940(3) Å in $\mathbf{2^O}$ is shorter than the 2.0226(19) Å in $\mathbf{2^N}$ (1.925 versus 1.994 Å at the BP86-D3/TZ2P level), which is consistent with the stronger π back-bonding of the OHC ligand.

Other Ir complexes are likewise accessible. For example, treating DBTOF with $[IrCl_2Cp^*]_2$ (Cp^* = pentamethylcyclopentadienyl) in refluxing toluene for 3 days gave orange OHC Ir(III) complex $\mathbf{3^O}$ quantitatively (Scheme 3, top). NHC complex $\mathbf{3^N}$ was obtained analogously in 88% yield, but SHC complex $\mathbf{3^S}$, like $\mathbf{2^S}$, could not be obtained, as DBTTF would not dissociate even after prolonged heating at 110 °C.

To access $\mathbf{3^S}$, we turned to the deprotonation route using the dithiolium salt.[21] Slow addition of the strong base potassium hexamethyldisilazide (KHMDS) to a mixture of commercially available benzodithiolium tetrafluoroborate and $[IrCl_2Cp^*]_2$ in THF led indeed to $\mathbf{3^S}$ in a remarkably high yield of 80%

https://dx.doi.org/10.1021/acs.organomet.0c00066
Organometallics 2020, 39, 1762−1771

Scheme 3. Synthesis of the Ir(III) Complexes 3^N, 3^O, and 3^S

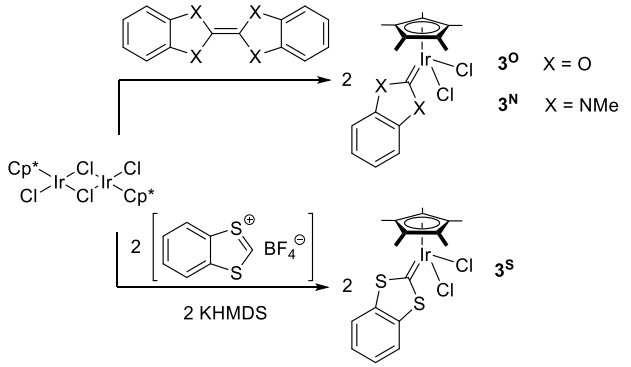

(Scheme 3, bottom); slow addition limits the formation of the carbene dimer. All three Ir(III) complexes 3^N, 3^O, and 3^S were characterized spectroscopically (see the Supporting Information). The ^{13}C NMR chemical shifts of the carbene carbon atom of 3^N, 3^O, and 3^S at δ 170.3, 197.9, and 231.1 ppm, respectively, are informative, as they reflect the increased π-acceptor ability of the carbene ligand on going from 1^N to 1^O to 1^S, which is in accord with the noted acceptor properties of the carbene ligands.[20,22]

The molecular structures of the complexes obtained by single-crystal X-ray diffraction measurements show surprisingly different spatial orientations (Figure 4).[23] The carbene ligand

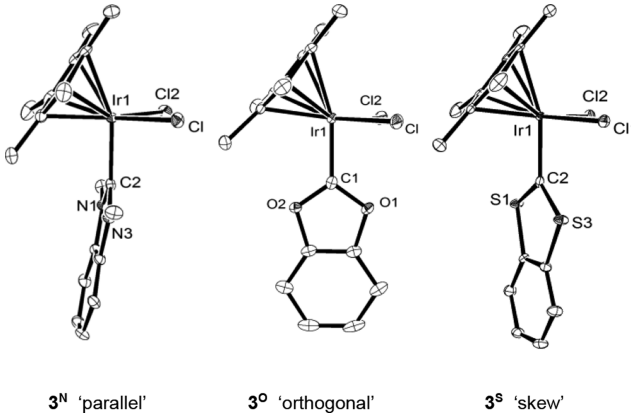

Figure 4. Structures of 3^N (left), 3^O (middle), and 3^S (right) in the crystal state. Ellipsoids are set at 50% probability; H atoms are omitted for clarity. Selected bond lengths (Å) and angles (deg): 3^N, Ir1−C2 2.027(4), N1−C2 1.358(6), N3−C2 1.366(5), N1−C2−N3 105.5(3), C2−Ir1−Cl2 91.50(12), Cl2−Ir1−Cl1 84.20(4); 3^O, Ir1−C1 1.9535(17), O2−C1 1.340(2), O1−C1 1.339(2), O1−C1−O2 109.58(14), C1−Ir1−Cl1 89.74(5), Cl2−Ir1−Cl1 88.414(16); 3^S, Ir1−C2 1.999(2), S1−C2 1.686(3), S3−C2 1.701(2), S2−C2−S3 114.08(14), C2−Ir1−Cl1 88.89(7), Cl2−Ir1−Cl1 88.95(2).

of 3^O is orthogonal to the Cp* ligand and has a rather short Ir−C bond of 1.9535(17) Å, whereas both ligands are aligned ("parallel") in 3^N, which has a longer Ir−C bond of 2.027(4) Å. These two structures have approximate C_s geometries, while 3^S has a "skewed" conformation with a 24° angle bisecting the planes of the ligands and an Ir−C bond length of 1.999(2) Å that is intermediate to those of the others. We conclude that the rotation of the carbene by 90° from 1^O to 1^N is sterically driven, as the *N*-methyl groups would interfere with the Cp* ring in an orthogonal arrangement.[24]

BP86-3D/TZ2P calculations corroborated this hypothesis, showing "parallel" 3^N to be favored over "orthogonal" $3^{N\prime}$ by a significant 12.5 kcal mol^{-1}; the N′ notation reflects the ligand's orthogonality. The two conformational isomers of both 3^O and 3^S were instead found to be approximately isoenergetic (see the Supporting Information). At this juncture it seemed relevant to examine the nature of the interaction of the carbene ligands (1^O, 1^S, and 1^N) with [$IrCl_2Cp^*$] in the "orthogonal" complexes by using an energy decomposition analysis at the BP86-D3/TZ2P level (C_s symmetry). For comparison, the Ir−carbene bond distances of $3^{N\prime}$ and 3^S were fixed to the equilibrium value of 3^O (1.906 Å) to eliminate the effect of steric interactions with the Cp* ligand. σ donation from the carbene lone pair into the empty metal d orbital dominates the bonding in all three complexes and is stronger for $3^{N\prime}$ and 3^S than for 3^O (Figure 5 and Table S3). π back-bonding from the

	ΔE^σ	ΔE^π	%π	$\Delta\varepsilon$	Sx10^{-1}	LUMO Carbene population
$3^{N'}$	-112.1	-24.4	18	3.46	0.63	0.08
3^O	-108.4	-34.0	24	2.49	1.01	0.25
3^S	-113.3	-35.5	24	2.15	1.24	0.37

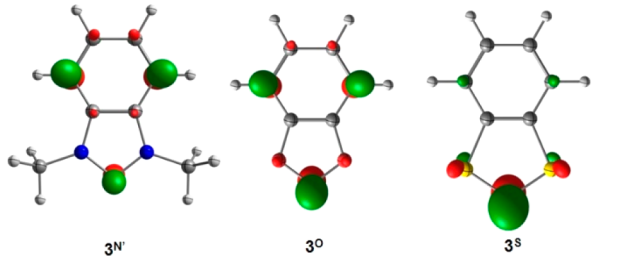

Figure 5. Principal fragment orbitals establishing the back-bonding contribution of the Ir−carbene bond for 3^N, 3^O, and 3^S in the orthogonal conformation (calculated with a Ir−C distance of 1.906 Å). Below the table are the LUMOs of $3^{N\prime}$ (left), 3^O (middle), and 3^S (right) with isocontour values of 0.07 au. Table columns: ΔE^σ (symmetrical a′) and ΔE^π (antisymmetrical a″) are the orbital interaction energy contributions in kcal mol^{-1}; % π is the relative π contribution, $\Delta\varepsilon$ is the HOMO (metal d)−LUMO (carbene p) energy gap of the fragments in eV, *S* is the orbital overlap, and the population of the carbene LUMO e (see the Supporting Information for details).

metal d_{xz} orbital into the LUMO of the carbene (p_π orbital) is instead stronger for 3^O (24%) and $3^{S\prime}$ (24%) than for $3^{N\prime}$ (18%) due the smaller energy gap and better overlap between the fragment orbitals (Figure 5). It appears that NHC π back-bonding is too modest to compensate the steric interaction in the orthogonal complex,[25] in concurrence with the experimentally observed and computationally favored parallel conformation of 3^N. The energy decomposition analysis further confirms the strong π-accepting property of both the OHC and SHC ligands, which is evident from the relative energy differences $\Delta\varepsilon$ and the $3^{N\prime} < 3^O < 3^S$ population of their carbene fragment orbitals.

In an attempt to quantify the net donation of the 1^N, 1^O, and 1^S ligands to the Ir(I) center, we turned to the Tolman electronic parameter, which reflects the ligand donor properties in the CO stretching frequencies of the metal carbonyl group. There are ample such parameters known for NHC TM complexes with excellent linear correlations. The difficulty is, of course, that a CO ligand is required at the Ir center.[5c,26]

https://dx.doi.org/10.1021/acs.organomet.0c00066
Organometallics 2020, 39, 1762−1771

We were able to obtain [IrCl(CO)$_2$1^N] (4^N; Figure 6), but exposure of [Ir(Cl)(cod)(2^O)] to CO led, unfortunately, to

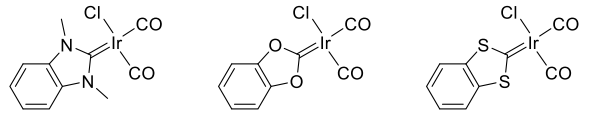

4^N TEP (calc.): 2044 cm^{-1} TEP (exp.): 2040 cm^{-1} | 4^O TEP (calc.): 2057 cm^{-1} | 4^S TEP (calc.): 2049 cm^{-1}

Figure 6. Complexes 4^N, 4^O, and 4^S together with their calculated and observed TEPs.

instant decomposition. This observation in itself illustrates the strong acceptor properties of 1^O. Since the TEP of (2040 cm^{-1} for 4^N compares well with the computed value of 2044 cm^{-1} (BP86-D3/TZ2P geometry), we would have expected a larger TEP for 4^O on the basis of its calculated value of 2057 cm^{-1}, which is in line with the stronger π-accepting property of 1^O. Finally, the computed TEP of 2049 cm^{-1} for 4^S indicates that the net donation of the SHC ligand lies between those of NHC and OHC, which agrees with the noted good π-acceptor and intermediate σ-donor capacity of 1^S (see the Supporting Information).

Cu, Ag, AND Au COMPLEXES

For the synthesis of the OHC and SHC coinage metal(I) complexes, we explored transmetalation, which required access to the unknown silver complexes. Whereas their synthesis by means of alkene dissociation seemed appealing, the reaction of DBTOF or DBTTF with silver(I) salts invariably led to elemental silver, probably due to olefin oxidation akin to tetra-N-alkenes and in line with electrochemical studies.[18,27] Instead, reacting benzodithiolium tetrafluoroborate with a slight excess of silver acetate afforded SHC silver complex 5^S in high (91%) yield (Scheme 4).[28] 5^S was fully characterized by NMR

Scheme 4. Synthesis of 5^S, 6^S, 7^S, and 8^S

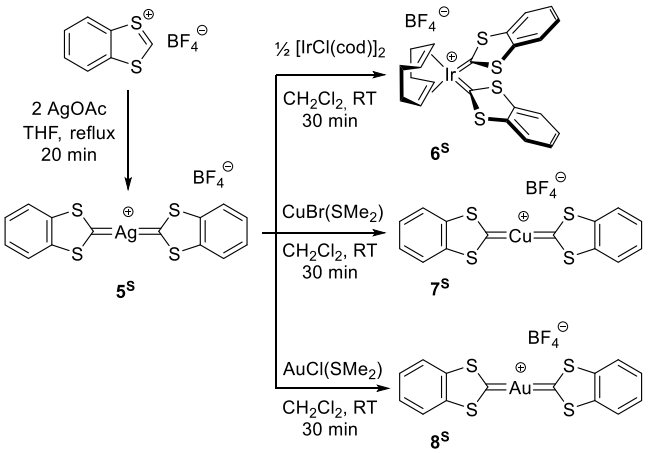

spectroscopy (see the Supporting Information). Its molecular structure, obtained by a single-crystal X-ray structure determination, shows the BF_4^- anion to be well separated from the cationic complex (the closest CH···F contact is 2.366 Å). The Ag^+ complex has approximate D_{2h} symmetry with two coplanar 1^S ligands and a C−Ag−C angle of 176.8(2)° (Figure 7, left). The Ag−carbene bond lengths of 2.115(7) and

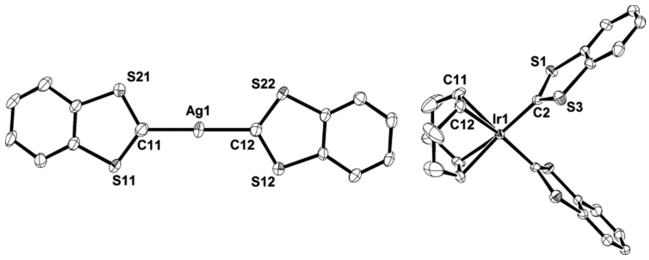

Figure 7. Structures of 5^S (left) and 6^S (right; only one of two independent molecules in the asymmetric unit is shown) in the crystal state Ellipsoids are set at 50% probability; counteranions, solvent molecules, and H atoms are omitted for clarity). Selected bond lengths (Å) and angles (deg) (those for the second molecule of 6^S are given in brackets): 5^S, Ag1−C11 2.115(7), Ag1−C12 2.103(6), C11−S11 1.667(8), C11−S21 1.664(7), C12−S22 1.672(7), C12−S12 1.667(7), C11−Ag−C12 176.8(2), S12−C12−S22 113.7(4), S11−C11−S21 114.2(4); 6^S, Ir1−C2 1.989(2) [1.991(5)], Ir1−C11 2.210(6) [2.229(5)], Ir1−C12 2.217(6) [2.202(5)], C11−C12 1.392(9) [1.382(8)], C2−S1 1.692(5) [1.694(5)], C2−S3 1.683(5) [1.680(6)], C2−Ir1−C2′ 88.8(3) [88.8(3)], S1−C2−S3 114.4(3) [114.0(3)].

2.103(6) Å are in the upper range of comparable bis-NHC-ligated Ag(I) complexes[29] and reflect weak metal−carbene interactions that are attributed to electronic factors, as the carbene ligands exercise no steric repulsion.

With 5^S in hand, its potential as a carbene transfer agent could be examined in analogy to the Ag-mediated NHC transfer reactions.[30] We first pursued iridium complex 2^S, the missing sulfur analogue of 2^O (see Scheme 2), by transferring one SHC ligand from 5^S to [IrCl(cod)]$_2$ but instead obtained bis-SHC complex 6^S (Scheme 4, top right) together with an equimolar amount of the unreacted Ir complex; employing 2 equiv of 5^S gave 6^S in 73% yield. The ^{1}H and ^{13}C NMR spectra reveal a highly symmetrical cod ligand and indicate the presence of two SHC ligands, which was confirmed by the molecular structure obtained from a single-crystal X-ray analysis (Figure 7, right). Whereas the reaction of the Ag complex 5^S with [IrCl(cod)]$_2$ did not yield Ir complex 2^S but instead Ir complex 6^S, the important conclusion is that the Ag^+ complex can serve as an SHC transmetallating complex.

To further validate the ability of 5^S to transfer its SHC carbene, we examined its exposure to Cu(I) and Au(I) salts. Reacting 5^S with an equimolar amount of [CuBr·SMe$_2$] or [AuCl·SMe$_2$] led to the coinage-metal bis-SHC complexes 7^S and 8^S in 74% and 88% yields, respectively (Scheme 4, right). Both complexes were characterized spectroscopically (see the Supporting Information), as no suitable crystals could be obtained for X-ray crystal structure determinations. The ^{13}C NMR chemical shifts of the carbene carbon atoms of 7^S and 8^S at δ 235.4 and 232.0 ppm, respectively, compare well with δ 231.1 for the Ir complex 3^S and reflect the strong π-acceptor ability of the SHC carbene ligand.

The bonding nature of the coinage metal complexes 5^S, 7^S, and 8^S was assessed at the BP86/TZ2P level using D_{2h}-optimized geometries. The lengths of the metal−carbene bonds (5^S, 2.071 Å; 7^S, 1.869 Å; 8^S, 2.020 Å) and their strengths (Ag < Cu < Au), as deduced from an energy decomposition analysis (Table 1), follow the commonly observed trends.[31] Silver complexes have the weakest bond, which concurs with their use as a transmetalation reagent. The bonding to the d^{10} group 11 metal cations are governed by electrostatic interactions[32] and are comparable to those of the

https://dx.doi.org/10.1021/acs.organomet.0c00066
Organometallics 2020, 39, 1762−1771

Table 1. Energy Decomposition Analyses and Bond Dissociation Energies (in kcal mol^{-1}) for the Coinage-Metal $(SHC)_2$ Complexes 5^S, 7^S, and 8^S and for the Gold NHC and OHC Complexes $[Au(1^N)_2]^+$ (8^N) and $[Au(1^O)_2]^+$ (8^O)

	5^S (Ag)	7^S (Cu)	8^S (Au)	8^N (Au)	8^O (Au)
$d_{M-carbene}$ (Å)	2.071	1.869	2.020	2.030	2.011
ΔE_σ (kcal mol^{-1})	−84.7	−96.6	−145.1	−143.2	−141.1
ΔE_π (kcal mol^{-1})	−23.1	−34.1	−32.3	−31.1	−32.0
ΔE_{bond} (kcal mol^{-1})	−152.2	−193.7	−215.0	−238.9	−205.4

$[M(CAAC)_2]^+$ (M = Cu, Ag, Au) complexes, which have been studied by Bertrand and Frenking[33] using the EDA-NOCV scheme and by Weinhold within the NBO model.[34] The main orbital contribution for the SHC complexes (5^S (Ag), 7^S (Cu), 8^S (Au); Table 1) is due to σ bonding from the carbene lone pair to the coinage-metal cations and is the strongest for Au due to the relativistic effect on the atomic orbitals, where the valence s and p orbitals are contracted and the d and f orbitals expanded.[32] However, the more distinguishing feature is the sizable π back-bonding of the SHC and OHC ligands (~32 kcal/mol; Table 1), as it is about twice that of CAAC.[32] In comparison to the NHC ligand, the SHC and OHC ligands both bind less strongly to Cu(I), Ag(I), and Au(I) (see Table 1 for the Au(I) complexes and the Supporting Information for a detailed bond energy analysis of all).

CONCLUSIONS

In summary, we report on the convenient syntheses of new OHC and SHC transition-metal complexes by (1) dissociation of a suitable olefin, (2) deprotonation of a precursor salt, or (3) transmetalation from a precursor Ag complex. The hitherto neglected OHCs and SHCs differ both electronically and sterically from the classical NHCs and thereby extend the panoply of available carbene ligands. Their strong π-accepting properties can be beneficial in synthetic and catalytic applications. Especially notable is the capability of 5^S to transfer the SHC ligand, allowing for facile access to a much wider range of carbene complexes. The applicability of the new benzannulated heterocyclic carbenes OHC 1^O and SHC 1^S is a target for further study.

EXPERIMENTAL SECTION

Materials and Methods. All reactions and manipulations were carried out under an atmosphere of dry nitrogen using standard Schlenk techniques or in a glovebox, unless otherwise stated. Dry, oxygen-free solvents were employed. Melting points were determined with samples in nitrogen-filled, sealed capillaries using a Büchi M-565 Melting Point apparatus and are uncorrected. Solution ^{1}H, ^{13}C, ^{11}B, ^{19}F, and ^{77}Se NMR spectra were recorded on Bruker Avance 250 (^{19}F), 400 (^{1}H, ^{13}C, ^{19}B, ^{77}Se) and 500 (^{1}H, ^{13}C) spectrometers at 298 K, unless otherwise stated. Chemical shifts (δ) are expressed with a positive sign, in parts per million. ^{1}H and ^{13}C chemical shifts reported were referenced internally to residual protio (1H) or deuterio (^{13}C) solvent,[35] while ^{11}B, ^{19}F, and ^{77}Se chemical shifts are relative to $BF_3{\cdot}Et_2O$, $CFCl_3$, and 0.25 mol/L KSeCN (aqueous, −329 ppm) external references, respectively. The following abbreviations and their combinations are used: br, broad; s, singlet; d, doublet; t, triplet; q, quartet, m, multiplet. The ^{1}H and ^{13}C resonance signals were attributed by means of 2D HSQC and HMBC experiments when necessary. Infrared spectra were recorded with a Shimadzu FT-IR 8400S spectrometer. Vibrational bands (ν) are expressed in cm^{-1}. Electrospray ionization (ESI) mass spectra were recorded on a Bruker Daltonics microTOF apparatus in positive ion mode (capillary potential of 4500 V). Benzo-1,3-dioxole-2-selone (1^O-**Se**),[17] dibenzotetraoxafulvalene,[17] pentamethylcyclopentadienyl iridium(III) chloride dimer ($[IrCl_2Cp^*]_2$),[36] and bis(1,3-dimethylbenzimidazolidin-2-ylidene)[37] were prepared according to reported procedures. All other starting materials were purchased from commercial vendors and used without further purification.

1^N-Se. This compound was prepared according to modified reported procedures.[38] NaHMDS (363 mg, 1.98 mmol, 1.1 equiv) in Et_2O (10 mL) was added via cannula to a dispersion of 1,3-dimethyl-1*H*-benzimidazolium iodide (493 mg, 1.8 mmol, 1.0 equiv) and Se powder (710 mg, 9 mmol, 5.0 equiv) in Et_2O (15 mL) at −78 °C. The cannula was rinsed with additional Et_2O (5 mL). After the reaction mixture was stirred for 20 min at −78 °C, the cold bath was removed and the suspension was stirred for 12 h and warmed to room temperature. The reaction mixture was filtered over a pad of Celite (3 cm) and silica gel (3 cm) on a filter frit. The frit was rinsed with additional Et_2O (20 mL). Volatiles were removed *in vacuo*. The resulting yellow residue was recrystallized from Et_2O to give 1^N-**Se** as yellow crystals. Yield: 135 mg (33%). Mp: 174−176 °C. ^{1}H NMR (400 MHz, $CDCl_3$): δ 7.57 (s, 4H, H_{Ar}), 3.89 (s, 6H, H_{CH3}). $^{13}C\{^1H\}$ NMR (100 MHz, $CDCl_3$) δ 166.9 (s, $C_{C=Se}$), 133.5 (s, C_{ArN}), 123.8 (s, C_{ArH}), 109.6 (s, C_{ArH}), 33.4 (s, C_{CH3}). $^{77}Se\{^1H\}$ NMR (76 MHz, $(CD_3)_2CO$): δ 80.0 (s). IR (ATR): ν 3094, 3043, 2962, 2085, 2004, 1454, 1383, 1333, 733. HRMS (ESI+): calcd for $[M + H]^+ = C_9H_{11}N_2Se^+$, 227.0082; found, 227.0074.

1^S-Se. NaHMDS (363 mg, 1.98 mmol, 1.1 equiv) in Et_2O (15 mL) was added via a cannula very slowly (ca. 30 min) to a dispersion of 1,3-dimethyl-1*H*-benzimidazolium iodide (493 mg, 1.8 mmol, 1.0 equiv) and Se powder (710 mg, 9 mmol, 5.0 equiv) in Et_2O (15 mL) at ambient temperature. The cannula was rinsed with additional Et_2O (2 mL). The gray suspension was stirred for 12 h. The reaction mixture was filtered over a pad of Celite (3 cm) and silica gel (3 cm) on a filter frit. The frit was rinsed with additional Et_2O (50 mL). Volatiles were removed *in vacuo*. The resulting orange residue was purified by column chromatography (silica gel, cyclohexane, R_f = 0.13) to give 1^S-**Se** as an orange crystalline powder. Yield: 37 mg (9%). The predominant byproduct of this reaction is dibenzotetrathiafulvalene. 1^S-**Se** decomposes slowly on the column during the chromatographic workup and when it is kept in solution. Mp: 219−220 °C dec (lit.[39] mp 214−216 °C). ^{1}H NMR (400 MHz, CD_2Cl_2): δ 7.61 (m, 2H, H_{Ar}), 7.35 (m, 2H, H_{Ar}). $^{13}C\{^1H\}$ NMR (100 MHz, CD_2Cl_2) δ 205.3 (s, $C_{C=Se}$), 145.3 (s, C_{ArS}), 127.9 (s, C_{ArH}), 121.9 (s, C_{ArH}). $^{77}Se\{^1H\}$ NMR (76 MHz, $(CD_3)_2CO$): δ 1017.2 (s). IR (ATR): ν 3047, 2955, 2922, 2853, 1431, 1261, 933, 906. HRMS (ESI+): calcd for $[M + H - Se]^+ = C_7H_5S_2^+$, 152.9827; found, 152.9828.

2^N. 1,3-Dimethyl-1*H*-benzimidazolium iodide (274.1 mg, 1.0 mmol, 1.0 equiv) and Ag_2O (115.9 mg, 0.5 mmol, 0.5 equiv) were transferred into a Schlenk flask, suspended in dichloromethane (5 mL), and stirred for 60 min at ambient temperature with exclusion of light. The iridium dimer complex $[Ir_2Cl_2(cod)_2]$ (336.0 mg, 0.5 mmol, 0.5 equiv) was added under a positive nitrogen flow. The yellow suspension was stirred for 4.5 h with exclusion of light and then filtered over a pad of Celite to give a clear dark yellow solution. Volatiles were removed *in vacuo*. The orange residue was purified in air by column chromatography (silica gel, eluent dichloromethane, R_f = 0.37) to give 2^N as a bright yellow crystalline solid. Crystals suitable for X-ray crystallography were grown at 4 °C by vapor diffusion of diethyl ether into a concentrated solution of 2^N in dichloromethane. Yield: 448 mg (93%). Mp: 188−191 °C dec. ^{1}H NMR (400 MHz, $CDCl_3$): δ 7.31−7.23 (m, 4H, H_4 and H_5), 4.74 (m, 2H, H_6 or H_9), 4.17 (s, 6H, H_2), 2.98 (m, 2H, H_6 or H_9), 2.30 (m, 4H, H_7 or H_8), 1.75 (m, 4H, H_7 or H_8). $^{13}C\{^1H\}$ NMR (100 MHz, $CDCl_3$): δ 192.0 (s, C_1), 135.6 (s, C_3), 122.7 (s, C_4 or C_5), 109.6 (s, C_4 or C_5), 87.0 (s, C_6 or C_9), 52.3 (s, C_6 or C_9), 34.4 (s, C_2), 33.7 (s, C_7 or C_8), 29.6 (s, C_7 or C_8); IR (ATR): ν 3026, 2928, 2878, 2827, 1489, 1436, 1342, 1094, 754, 744, 565. HRMS (ESI+): calcd for $[M - Cl]^+ = C_{17}H_{22}N_2Ir^+$, 447.1407; found, 447.1392.

2^O. The iridium dimer complex $[Ir_2Cl_2(cod)_2]$ (357 mg, 0.53 mmol, 1.0 equiv) and dibenzotetraoxafulvalene (166 mg, 0.69 mmol, 1.3 equiv) were transferred into a Schlenk flask and solubilized in toluene (6 mL). The mixture was stirred at room temperature for 4

https://dx.doi.org/10.1021/acs.organomet.0c00066
Organometallics 2020, 39, 1762−1771

days. Over time, the media changed gradually from orange to brown. Volatiles were removed *in vacuo*, and the residue was washed with diethyl ether (8 × 5 mL) to remove starting material and byproducts; the product is also slightly soluble in diethyl ether. The remaining red-orange solid was dried under vacuum to give $\mathbf{2^O}$. Yield: 280 mg (58%). Crystals suitable for X-ray crystallography were grown at room temperature by vapor diffusion of diethyl ether into a solution of $\mathbf{2^O}$ in dichloromethane. The compound decomposes under nitrogen and only slowly (over days) in solution at room temperature, as indicated by formation of a black insoluble residue. Mp: 115−117 °C dec. ^{1}H NMR (400 MHz, $CDCl_3$): δ 7.55 (m, 2H, H_3 or H_4), 7.40 (m, 2H, H_3 or H_4), 5.53 (m, 2H, H_8), 3.52 (m, 2H, H_5), 2.60 (m, 8H, H_6 and H_7). $^{13}C\{^1H\}$ NMR (100 MHz, $CDCl_3$) δ 209.2 (s, C_1), 146.7 (s, C_2), 126.5 (s, C_3 or C_4), 111.8 (s, C_3 or C_4), 104.7 (s, C_8), 56.1 (s, C_5), 33.6 (s, C_6 or C_7), 29.4 (s, C_6 or C_7). IR (ATR): ν 3097, 3057, 3018, 2952, 2880, 2833, 1466, 1333, 1194, 1049, 746. HRMS (ESI+): calcd for $[M - Cl]^+ = C_{15}H_{16}O_2Ir^+$, 421.0774; found, 421.0785.

$\mathbf{3^N}$. A solution of bis(1,3-dimethylbenzimidazolidin-2-ylidene) (29.2 mg, 0.10 mmol, 1.0 equiv) in toluene (1 mL) was added to a solution of $[IrCl_2Cp^*]_2$ (79.7 mg, 0.10 mmol, 1.0 equiv) in toluene (1 mL). The reaction mixture was stirred for 4 h at 100 °C and then for 2 days at room temperature in order to ensure full conversion and limit thermal decomposition. The resulting yellow precipitate was isolated by filtration, washed with diethyl ether (3 × 2 mL), and dried under vacuum to give $\mathbf{3^N}$. Yield: 95 mg (88%). Crystals suitable for X-ray crystallography were grown at room temperature by vapor diffusion of pentane into a solution of $\mathbf{3^N}$ in dichloromethane. Mp: 334 °C. ^{1}H NMR (400 MHz, $CDCl_3$): δ 7.37 (m, 2H, H_3 or H_4), 7.30 (m, 2H, H_3 or H_4), 4.17 (s, 6H, H_{N-CH3}), 1.68 (s, 15H, H_{Cp^*-CH3}). $^{13}C\{^1H\}$ NMR (100 MHz, $CDCl_3$) δ 170.25 (s, C_1), 135.87 (s, C_2), 123.49 (s, C_3 or C_4), 110.35 (s, C_3 or C_4), 89.61 (s, C_{Cp^*}), 35.60 (s, C_{N-CH3}), 9.35 (s, C_{Cp^*-CH3}). IR (ATR): ν 1444, 1375, 1344, 1093, 767. HRMS (ESI+): calcd for $[M - Cl]^+ = C_{19}H_{25}ClN_2Ir^+$, 509.1330; found, 509.1330.

$\mathbf{3^O}$. The iridium dimer complex $[IrCl_2Cp^*]_2$ (199 mg, 0.25 mmol, 1.0 equiv) and dibenzotetraoxafulvalene (60 mg, 0.25 mmol, 1 equiv) were transferred into a pressurizable Schlenk flask (featuring a screw cap) and dispersed in toluene (6 mL). The mixture was heated at 110 °C with vigorous stirring. Over time, the media changed from red to yellow. After 64 h, the mixture was cooled to room temperature. The yellow-orange residue was isolated by cannula filtration, washed with Et_2O (3 × 3 mL), and subsequently dried *in vacuo*. Yield: 258 mg (quantitative). Crystals suitable for X-ray crystallography were grown at room temperature by vapor diffusion of pentane into a concentrated solution of $\mathbf{3^O}$ in dichloromethane. Mp: 139−204 °C dec. ^{1}H NMR (400 MHz, $CDCl_3$): δ 7.65 (m, 2H, H_{ar}), 7.43 (m, 2H, H_{ar}), 1.84 (s, 15H, H_{CH3-Cp^*}). $^{13}C\{^1H\}$ NMR (100 MHz, $CDCl_3$): δ 197.9 (s, C_1), 147.3 (s, C_2), 126.8 (s, C_4), 111.9 (s, C_3), 95.8 (s, C_{Ar-Cp^*}), 9.2 (s, C_{CH3-Cp^*}). IR (ATR): ν 3086, 3058, 2916, 1458, 1199, 793, 758. HRMS (ESI+): calcd for $[M - Cl]^+ = C_{17}H_{19}ClIrO_2^+$, 483.0703; found, 483.0689.

$\mathbf{3^S}$. To a solution of the iridium dimer complex $[IrCl_2Cp^*]_2$ (150 mg, 0.19 mmol, 1.0 equiv) and benzodithiolium tetrafluoroborate (180.8 mg, 0.75 mmol, 4.0 equiv) in dichloromethane (15 mL) was slowly added at 0 °C a solution of KHMDS (150.2 mg, 0.75 mmol, 4.0 equiv) in tetrahydrofuran (15 mL) by means of a syringe pump over 160 min. Slow addition of the thiazolium salt is mandatory to avoid extensive formation of the corresponding carbene dimer. After the addition was finished, the mixture was warmed to room temperature, volatiles were removed under vacuum, and the residue was washed with diethyl ether (4 × 5 mL) and benzene (2 × 4 mL) and dried under vacuum to yield $\mathbf{3^S}$ as a yellow-orange powder. Yield: 164 mg (80%). Crystals suitable for X-ray crystallography were grown at room temperature by vapor diffusion of pentane into a concentrated solution of $\mathbf{3^S}$ in dichloromethane. Mp: >195−265 °C dec. ^{1}H NMR (400 MHz, CD_2Cl_2): δ 8.11 (m, 2H, H_{ar}), 7.56 (m, 2H, H_{ar}), 1.68 (s, 15H, H_{CH3-Cp^*}). $^{13}C\{^1H\}$ NMR (100 MHz, $CDCl_3$): δ 231.1 (s, C_1), 150.1 (s, C_2), 127.5 (s, C_4), 123.3 (s, C_3), 92.8 (s, C_{Ar-Cp^*}), 8.7 (s, C_{CH3-Cp^*}). IR (ATR): ν 3061, 2983, 2964, 2918, 1751, 1491, 1435, 1421, 1400, 1373, 1027, 939, 875, 777. HRMS (ESI+): calcd for $[M - Cl]^+ = C_{17}H_{19}ClIrS_2^+$, 515.0230; found, 515.0205.

$\mathbf{4^N}$. Iridium NHC(COD) complex $\mathbf{2^N}$ (55 mg, 0.11 mmol, 1.0 equiv) was transferred into a Schlenk flask and solubilized in dichloromethane (25 mL). CO gas was bubbled through the solution for 10 min. Volatiles were removed *in vacuo*. The yellow residue was washed with pentane (3 × 2 mL) and dried under vacuum to give $\mathbf{4^N}$ as a microcrystalline yellow powder. Yield: 43 mg (91%). Mp: 158−159 °C dec. ^{1}H NMR (500 MHz, CD_2Cl_2): δ 7.49 (m, 2H, H_4 or H_5), 7.43 (m, 2H, H_4 or H_5), 4.10 (s, 6H, H_2). $^{13}C\{^1H\}$ NMR (126 MHz, CD_2Cl_2) δ 183.4 (s, C_1), 182.3 (s, CO_{trans}), 168.5 (s, CO_{cis}), 135.1 (s, C_3), 124.4 (s, C_4 or C_5), 111.1 (s, C_4 or C_5), 35.4 (s, C_2). IR (ATR): ν 2947, 2054, 1969, 1456, 1383, 1130, 1094, 766, 743. HRMS (ESI+): calcd for $[M + H]^+ = C_{11}H_{11}ClIrN_2O_2^+$, 431.0125; found, 431.0129.

$\mathbf{5^S}$. Benzodithiolium tetrafluoroborate (500 mg, 2.08 mmol, 1.0 equiv) and silver(I) acetate (695.3 mg, 4.17 mmol, 2.0 equiv) were suspended in THF (30 mL) and heated to reflux for 20 min. After it was cooled to room temperature, the green reaction mixture was filtered by cannula filtration. The remaining dark gray residue was washed with THF (2 × 5 mL) and extracted into acetonitrile (6 × 5 mL). During the extraction, the receiving flask was cooled to −78 °C in order to freeze the acetonitrile solution and avoid decomposition. Volatiles were removed under vacuum at room temperature to give $\mathbf{5^S}$ as a gray solid. Yield: 473 mg (91%). Crystals of poor but sufficient quality for X-ray crystallography were grown at 4 °C by vapor diffusion of hexanes into a concentrated solution of $\mathbf{5^S}$ in dichloromethane. Slightly longer reflux times (e.g., 40 min) during the synthesis resulted in complete decomposition. The compound was moderately stable in chlorinated solvents but decomposed rapidly (mostly to dibenzotetrathiofulvalene and an unknown insoluble residue) in the presence of coordinating solvents such as acetonitrile or THF and was best stored in the solid state at −20 °C in the dark.[40] Mp: >70 °C dec. ^{1}H NMR (400 MHz, CD_3CN): δ 8.55 (m, 4H, H_3 or H_4), 7.82 (m, 4H, H_3 or H_4). $^{13}C\{^1H\}$ NMR (100 MHz, CD_3CN): δ 150.6 (s, C_2), 129.3 (s, C_3 or C_4), 125.2 (s, C_3 or C_4), C_1 not detected. $^{11}B\{^1H\}$ NMR (128 MHz, CD_3CN): δ −1.2 (s, BF_4). $^{19}F\{^1H\}$ NMR (235 MHz, CD_3CN): δ −151.7 (s). IR (ATR): ν 3090, 3055, 1439, 1427, 1088, 1030, 964, 950, 758. HRMS (ESI+): calcd for $[M - BF_4]^+ = C_{14}H_8AgS_4^+$, 410.8554; found, 410.8548.

$\mathbf{6^S}$. The iridium dimer complex (67.3 mg, 0.1 mmol, 1.0 equiv) and $\mathbf{5^S}$ (100.0 mg, 0.2 mmol, 2.0 equiv) were suspended in dichloromethane (8 mL) and stirred at ambient temperature for 30 min. The brown reaction mixture was filtered over a pad of Celite which was subsequently rinsed with dichloromethane (20 mL). The clear brown solution was concentrated under vacuum to a volume of ca. 2 mL. Addition of pentane (20 mL) led to the precipitation of a solid which was isolated by cannula filtration, washed with diethyl ether (3 × 3 mL), and dried under vacuum to give $\mathbf{6^S}$ as a dark brown solid. Yield: 100 mg (73%). Crystals suitable for X-ray crystallography were grown at 4 °C by layering a concentrated solution of $\mathbf{6^S}$ in fluorobenzene/dichloromethane (1/1) with fluorobenzene. Mp: >120 °C dec. ^{1}H NMR (400 MHz, $CDCl_3$): δ 8.21−8.16 (m, 4H, H_3 or H_4), 7.61−7.56 (m, 4H, H_3 or H_5), 4.52 (m, 4H, H_5), 2.65−2.48 (m, 8H, H_6). $^{13}C\{^1H\}$ NMR (100 MHz, $CDCl_3$): δ 240.6 (s, C_1), 147.1 (s, C_2), 128.0 (s, C_3 or C_4), 123.9 (s, C_3 or C_4), 90.7 (s, C_5), 31.8 (s, C_6). $^{11}B\{^1H\}$ NMR (128 MHz, $CDCl_3$): δ −0.7 (s, BF_4). $^{19}F\{^1H\}$ NMR (235 MHz, $CDCl_3$): δ −152.8. IR (ATR): ν 3090, 3045, 2955, 2881, 2837, 1435, 1026, 926, 847, 752. HRMS (ESI+): calcd for $[M - BF_4]^+ = C_{15}H_{16}IrS_2^+$, 453.0314; found, 453.0310.

$\mathbf{7^S}$. Dichloromethane (10 mL) was slowly added to a copper bromide dimethyl sulfide complex (41.2 mg, 0.2 mmol, 1.0 equiv) and $\mathbf{5^S}$ (100 mg, 0.2 mmol, 1.0 equiv) and stirred at ambient temperature for 30 min. The green reaction mixture was filtered over a pad of Celite. The clear dark green solution was evaporated to dryness. The brown residue was washed with diethyl ether (3 × 2 mL) and dried under vacuum to give $\mathbf{7^S}$ as a brown solid. Yield: 67 mg (74%). Mp: >85−120 °C dec. ^{1}H NMR (400 MHz, CD_2Cl_2): δ 8.49−8.47 (m, 4H, H_3 or H_4), 7.84−7.82 (m, 4H, H_3 or H_4). $^{13}C\{^1H\}$ NMR (100 MHz, CD_2Cl_2) δ 235.4 (s, C_1), 149.7 (s, C_2), 129.1 (s, C_3 or C_4),

https://dx.doi.org/10.1021/acs.organomet.0c00066
Organometallics 2020, 39, 1762−1771

124.5 (s, C_3 or C_4). $^{11}B\{^1H\}$ NMR (128 MHz, CD_2Cl_2): δ −0.83 (s). $^{19}F\{^1H\}$ NMR (235 MHz, CD_2Cl_2): δ −150.5 (s). IR (ATR): ν 3069, 3055, 1439, 1429, 1340, 1285, 1095, 948, 760. HRMS (ESI+): calcd for $[M - BF_4]^+ = C_{14}H_8CuS_4^+$, 366.8799; found, 366.8792.

8^S. A gold chloride dimethyl sulfide complex (29.5 mg, 0.1 mmol, 1.0 equiv) and 5^S (50 mg, 0.1 mmol, 1.0 equiv) were suspended in dichloromethane and stirred at ambient temperature for 30 min. The green reaction mixture was filtered via cannula. The clear dark green solution was concentrated under vacuum to a volume of ca. 1 mL. Addition of pentane (10 mL) led to the precipitation of a solid which was isolated by cannula filtration, washed with diethyl ether (3 × 3 mL), and dried under vacuum to give 8^S as a gray-greenish solid. Yield: 52 mg (88%). Mp: 110−140 °C dec. ^1H NMR (400 MHz, CD_2Cl_2): δ 8.53 (m, 4H, H_3 or H_4), 7.94 (m, 4H, H_3 or H_4). $^{13}C\{^1H\}$ NMR (100 MHz, CD_2Cl_2): δ 232.0 (s, C_1), 147.6 (s, C_2), 129.9 (s, C_3 or C_4), 125.2 (s, C_3 or C_4). $^{11}B\{^1H\}$ NMR (128 MHz, CD_2Cl_2): δ −1.1 (s, BF_4). $^{19}F\{^1H\}$ NMR (235 MHz, CD_2Cl_2): δ −151.1 (sbr, BF_4). IR (ATR): ν 3099, 3056, 1549, 1433, 1326, 1312, 1286, 1259, 1095, 1034, 758. HRMS (ESI+): calcd for $[M - BF_4]^+ = C_{14}H_8AuS_4^+$, 500.9169; found, 500.9188.

Computational Details. Calculations on the free carbenes were performed at the DFT B3LYP/TZVP level of theory using Gaussian09, Revision A.02.[41,42] Those on the carbene metal complexes were performed using the parallelized Amsterdam density functional (ADF) package (version 2014.04).[43] The Kohn−Sham MOs were expanded in a large, uncontracted basis set of Slater-type orbitals (STOs), of a triple-ζ basis set with two polarization function quality, corresponding to basis set TZ2P in the ADF package. All calculations were performed at the nonlocal exchange self-consistent field (NL-SCF) level, using the local density approximation (LDA) in the Vosko−Wilk−Nusair parametrization[44] with nonlocal corrections for exchange (Becke88)[45] and correlation (Perdew86)[46] and with Grimme-type dispersion correction (D3-BJ).[47] All geometries were optimized using the analytical gradient method implemented by Versluis and Ziegler,[48] including relativistic effects by the zeroth-order regular approximation (ZORA).[49]

The bonding interactions of the transition-metal to ligand bonds were analyzed with the ADF implemented energy decomposition[50] into an exchange (or Pauli) repulsion (ΔE_{Pauli}) between the electrons on the two fragments plus an electrostatic interaction energy part (ΔE_{elstat}) and an orbital interaction energy (charge transfer, polarization) part (ΔE_{orb}). The energy necessary to convert fragments from their ground-state equilibrium geometries to the geometry and electronic state they acquire in the complex is represented by a preparation energy term (ΔE_{prep}). The overall bond energy (ΔE_{tot}) is formulated as

$$\Delta E_{tot} = \Delta E_{Pauli} + \Delta E_{elstat} + \Delta E_{orb} + \Delta E_{prep}$$

Note that ΔE_{tot} is defined as the negative of the bond dissociation energy (BDE), i.e. $\Delta E_{tot} = E(\text{molecule}) - \sum E(\text{fragments})$, thereby resulting in negative values for stable bonds. The orbital interaction term ΔE_{orb} accounts for interactions between occupied orbitals on one fragment with unoccupied orbitals on the other fragment, including HOMO−LUMO interactions and polarization (empty/occupied orbital mixing on the same fragment). The charge transfer part is the result of both σ donation from the ligand to the metal and π back-donation from the metal into the unoccupied orbitals of the ligand. Instead of separating the charge transfer and polarization parts, we used the extended transition state (ETS) method developed by Ziegler and Rauk to decompose ΔE_{orb} into contributions from each irreducible representation of the interacting system.[50]

X-ray Structure Determination. The crystal structures were determined on a Bruker D8 Venture diffractometer with Photon100 detector at 123(2) K using Mo Kα radiation (2^O, 2^N, 3^N, 3^O, 3^S, 6^S) (0.71073 Å). Direct methods (2^O, 3^O, 6^S) or Patterson methods (2^N, 3^N, 3^S) were used for structure solution (SHELXS-97).[51] Refinement was carried out using SHELXL-2014 (full-matrix least-squares on F^2),[52] and hydrogen atoms were localized by difference Fourier synthesis and refined using a riding model. Semiempirical absorption corrections were applied for the compounds. For 2^O, 2^N, 3^N, 3^O, and 3^S extinction corrections were applied.[53] 3^N was refined as a two-component inversion twin (BASF = 0.277(7)). In 6^S one solvent molecule is disordered about a 2-fold axis (see cif file for details). CCDC 1451141 (2^O), CCDC 1451142 (2^N), CCDC 1451143 (3^N), CCDC 1451144 (3^O), CCDC 1451145 (3^S), CCDC 1451203 (5^S), and 1451146 (6^S) contain the supplementary crystallographic data for this paper. Additional crystallographic information is available in the Supporting Information.

■ ASSOCIATED CONTENT

Supporting Information

The Supporting Information is available free of charge at https://pubs.acs.org/doi/10.1021/acs.organomet.0c00066.

NMR spectra, additional computational details and crystallographic data, geometries of computed structures (PDF)

Computed Cartesian coordinates (XYZ)

Accession Codes

CCDC 1451141−1451146 and 1451203 contain the supplementary crystallographic data for this paper. These data can be obtained free of charge via www.ccdc.cam.ac.uk/data_request/cif, or by emailing data_request@ccdc.cam.ac.uk, or by contacting The Cambridge Crystallographic Data Centre, 12 Union Road, Cambridge CB2 1EZ, UK; fax: +44 1223 336033.

■ AUTHOR INFORMATION

Corresponding Author

Koop Lammertsma − *Department of Chemistry and Pharmaceutical Sciences, Faculty of Science, Vrije Universiteit Amsterdam, 1081 HV Amsterdam, The Netherlands; Department of Chemistry, University of Johannesburg, Johannesburg 2006, South Africa;* orcid.org/0000-0001-9162-5783; Email: K.Lammertsma@vu.nl

Authors

Maximilian Joost − *Department of Chemistry and Pharmaceutical Sciences, Faculty of Science, Vrije Universiteit Amsterdam, 1081 HV Amsterdam, The Netherlands*

Martin Nieger − *Laboratory of Inorganic Chemistry, Department of Chemistry, University of Helsinki, Helsinki, Finland*

Martin Lutz − *Crystal and Structural Chemistry, Bijvoet Center for Biomolecular Research, Utrecht University, 3584 CH Utrecht, The Netherlands*

Andreas W. Ehlers − *Department of Chemistry and Pharmaceutical Sciences, Faculty of Science, Vrije Universiteit Amsterdam, 1081 HV Amsterdam, The Netherlands; Van 't Hoff Institute for Molecular Sciences, University of Amsterdam, 1090 GD Amsterdam, The Netherlands; Department of Chemistry, University of Johannesburg, Johannesburg 2006, South Africa*

J. Chris Slootweg − *Department of Chemistry and Pharmaceutical Sciences, Faculty of Science, Vrije Universiteit Amsterdam, 1081 HV Amsterdam, The Netherlands; Van 't Hoff Institute for Molecular Sciences, University of Amsterdam, 1090 GD Amsterdam, The Netherlands;* orcid.org/0000-0001-7818-7766

Complete contact information is available at: https://pubs.acs.org/10.1021/acs.organomet.0c00066

Notes

The authors declare no competing financial interest.

https://dx.doi.org/10.1021/acs.organomet.0c00066
Organometallics 2020, 39, 1762−1771

■ ACKNOWLEDGMENTS

This work was supported by The Netherlands Organisation for Scientific Research, Chemical Sciences (NWO-CW). We acknowledge SARA Computing and Networking Services for computer time.

■ REFERENCES

(1) (a) Arduengo, A. J.; Harlow, R. L.; Kline, M. A Stable Crystalline Carbene. *J. Am. Chem. Soc.* **1991**, *113*, 361−363. (b) Hahn, F. E.; Jahnke, M. C. Heterocyclic Carbenes: Synthesis and Coordination Chemistry. *Angew. Chem., Int. Ed.* **2008**, *47*, 3122−3172; *Angew. Chem.* **2008**, *120*, 3166−3216. (c) *N-Heterocyclic Carbenes*; Díez-González, S., Ed.; Royal Society of Chemistry: Cambridge, U.K., 2010. (d) Hopkinson, M. N.; Richter, C.; Schedler, M.; Glorius, F. An Overview of N-Heterocyclic Carbenes. *Nature* **2014**, *510*, 485−496.

(2) (a) Melaimi, M.; Soleilhavoup, M.; Bertrand, G. Stable Cyclic Carbenes and Related Species beyond Diaminocarbenes. *Angew. Chem., Int. Ed.* **2010**, *49*, 8810−8849; *Angew. Chem.* **2010**, *122*, 8992−9032. (b) Wang, Y.; Robinson, G. H. N-Heterocyclic Carbene—Main-Group Chemistry: A Rapidly Evolving Field. *Inorg. Chem.* **2014**, *53*, 11815−11832.

(3) (a) Trnka, T. M.; Grubbs, R. H. CHR Olefin Metathesis Catalysts: An Organometallic Success Story. *Acc. Chem. Res.* **2001**, *34*, 18−29. (b) Glorius, F. *N-Heterocyclic Carbenes in Transition Metal Catalysis*; Springer Science & Business Media: 2007. (c) Enders, D.; Niemeier, O.; Henseler, A. Organocatalysis by N-Heterocyclic Carbenes. *Chem. Rev.* **2007**, *107*, 5606−5655. (d) Díez-González, S.; Marion, N.; Nolan, S. P. N-Heterocyclic Carbenes in Late Transition Metal Catalysis. *Chem. Rev.* **2009**, *109*, 3612−3676. (e) Cazin, C. S. J. *N-Heterocyclic Carbenes in Transition Metal Catalysis and Organocatalysis*; Springer Science & Business Media: 2010.

(4) Mercs, L.; Albrecht, M. Beyond Catalysis: N-Heterocyclic Carbene Complexes as Components for Medicinal, Luminescent, and Functional Materials Applications. *Chem. Soc. Rev.* **2010**, *39*, 1903−1912.

(5) (a) Mercs, L.; Labat, G.; Neels, A.; Ehlers, A. W.; Albrecht, M. Piano-Stool Iron(II) Complexes as Probes for the Bonding of N-Heterocyclic Carbenes: Indications for π-Acceptor Ability. *Organometallics* **2006**, *25*, 5648−5656. (b) Jacobsen, H.; Correa, A.; Poater, A.; Costabile, C.; Cavallo, L. Understanding the M-(NHC) (NHC = N-Heterocyclic Carbene) Bond. *Coord. Chem. Rev.* **2009**, *253*, 687−703. (c) Nelson, D. J.; Nolan, S. P. Quantifying and Understanding the Electronic Properties of N-Heterocyclic Carbenes. *Chem. Soc. Rev.* **2013**, *42*, 6723−6753. (d) Alcarazo, M.; Stork, T.; Anoop, A.; Thiel, W.; Fürstner, A. Steering the Surprisingly Modular π-Acceptor Properties of N-Heterocyclic Carbenes: Implications for Gold Catalysis. *Angew. Chem., Int. Ed.* **2010**, *49*, 2542−2546; *Angew. Chem.* **2010**, *122*, 2596−2600.

(6) (a) Würtz, S.; Glorius, F. Surveying Sterically Demanding N-Heterocyclic Carbene Ligands with Restricted Flexibility for Palladium-catalyzed Cross-Coupling Reactions. *Acc. Chem. Res.* **2008**, *41*, 1523−1533. (b) Droge, T.; Glorius, F. The Measure of All Rings-N-Heterocyclic Carbenes. *Angew. Chem., Int. Ed.* **2010**, *49*, 6940−6952; Das Maß aller Ringe - N-heterocyclische Carbene. *Angew. Chem.* **2010**, *122*, 7094−7107. (c) Benhamou, L.; Chardon, E.; Lavigne, G.; Bellemin-Laponnaz, S.; César, V. Synthetic Routes to N-Heterocyclic Carbene Precursors. *Chem. Rev.* **2011**, *111*, 2705−2733.

(7) Soleilhavoup, M.; Bertrand, G. Cyclic (Alkyl)(Amino)Carbenes (CAACs): Stable Carbenes on the Rise. *Acc. Chem. Res.* **2015**, *48*, 256−266.

(8) Rao, B.; Tang, H.; Zeng, X.; Liu, L.; Melaimi, M.; Bertrand, G. Cyclic (Amino)(aryl)carbenes (CAArCs) as Strong σ-Donating and π-Accepting Ligands for Transition Metals. *Angew. Chem., Int. Ed.* **2015**, *54*, 14915−14919; *Angew. Chem.* **2015**, *127*, 15128−15132.

(9) (a) Plaia, U.; Stolzenberg, H.; Fehlhammer, W. P. Homoleptic Carbene Complexes. 3. Hexakis(oxazolidin-2-ylidene)cobalt(III) and -rhodium(III). *J. Am. Chem. Soc.* **1985**, *107*, 2171−2172. (b) Tamm, M.; Ekkehardt Hahn, F. Reactions of β-Functional Phenyl Isocyanides. *Coord. Chem. Rev.* **1999**, *182*, 175−209. (c) Lindner, R.; Wagner, C.; Steinborn, D. Synthesis of Trimethylplatinum(IV) Complexes with N, N- and N, O-Heterocyclic Carbene Ligands and Their Reductive C-C Elimination Reactions. *J. Am. Chem. Soc.* **2009**, *131*, 8861−8874. (d) Bellemin-Laponnaz, S. Synthesis of N, O-Heterocyclic Carbene and Coordination to Rhodium(I) and Copper-(I). *Polyhedron* **2010**, *29*, 30−33.

(10) (a) Cardin, D. J.; Cetinkaya, B.; Cetinkaya, E.; Lappert, M. F. Carbene Complexes. Part I. Electron-rich Olefins as a Source of Carbene Complexes of Platinum(II) and Palladium(II); and Some Experiments with $(CF_3)_2CN_2$. *J. Chem. Soc., Dalton Trans.* **1973**, 514−522. (b) Raubenheimer, H. G.; Kruger, G. J.; Van A. Lombard, A.; Linford, L.; Viljoen, J. C. Sulfur-Containing Metal Complexes. 12. Reactions of α-Thio Carbanions with Carbene Complexes of the Type $[M(CO)_5\{O(alkyl)Ar\}]$ and with the Carbyne $[(\eta^5\text{-}MeC_5H_4)\text{-}Mn(CO)_2(CPh)][BCl_4]$. *Organometallics* **1985**, *4*, 275−284. (c) Johnson, L.; Angelici, R. J. Synthesis of Aminooxycarbene Complexes of Iron with N-Alkyl, -Allyl, -Carbamoyl Groups. *Inorg. Chem.* **1987**, *26*, 973−976. (d) Bertani, R.; Mozzon, M.; Michelin, R. A. Reactions of Aziridine, Thiirane, and Oxirane with Isocyanide Ligands in Complexes of Palladium(II) and Platinum(II): Syntheses of Neutral Five-Membered Cyclic Diamino-, Aminothio-, and Aminooxycarbene Compounds. *Inorg. Chem.* **1988**, *27*, 2809−2815. (e) Arduengo, A. J.; Goerlich, J. R.; Marshall, W. J. A Stable Thiazol-2-ylidene and Its Dimer. *Liebigs Ann.* **1997**, *1997*, 365−374. (f) Caló, V.; Sole, R. D.; Nacci, A.; Schingaro, E.; Scordari, F. Synthesis and Crystal Structure of Bis(2,3-dihydro-3-methylbenzothiazole-2-ylidene)palladium(II) Diiodide: The First Palladium Complex with Benzothiazole Carbene Ligands Suitable for Homogeneous Catalysis. *Eur. J. Org. Chem.* **2000**, *2000*, 869−871. (g) Caló, V.; Nacci, A.; Monopoli, A.; Spinelli, M. Arylation of Allylic Alcohols in Ionic Liquids Catalysed by a Pd-Benzothiazole Carbene Complex. *Eur. J. Org. Chem.* **2003**, *2003*, 1382−1385. (h) Enders, D.; Balensiefer, T. Nucleophilic Carbenes in Asymmetric Organocatalysis. *Acc. Chem. Res.* **2004**, *37*, 534−541. (i) Huynh, H. V.; Meier, N.; Pape, T.; Hahn, F. E. Benzothiazolin-2-ylidene Complexes of Iridium(I). *Organometallics* **2006**, *25*, 3012−3018. (j) Chien, S. W.; Yen, S. K.; Hor, T. S. A. N, S-Heterocyclic Carbene Complexes. *Aust. J. Chem.* **2010**, *63*, 727−741.

(11) (a) Hahn, F. E. Heterocyclic Carbenes. *Angew. Chem., Int. Ed.* **2006**, *45*, 1348−1352; *Angew. Chem.* **2006**, *118*, 1374−1378. (b) de Fremont, F.; Marion, N.; Nolan, S. P. Carbenes: synthesis, properties, and organometallic chemistry. *Coord. Chem. Rev.* **2009**, *253*, 862−892. (c) Kuwata, S.; Hahn, F. E. Complexes bearing protic N-heterocyclic carbene ligands. *Chem. Rev.* **2018**, *118*, 9642−9677.

(12) Taxak, N.; Patel, B.; Bharatam, P. V. Carbene Generation by Cytochromes and Electronic Structure of Heme-Iron-Porphyrin-Carbene Complex: A Quantum Chemical Study. *Inorg. Chem.* **2013**, *52*, 5097−5109.

(13) (a) Green, M.; Moss, J. R.; Nowell, I. W.; Stone, F. G. A. Synthesis of Manganese(I) Carbene Complexes. *J. Chem. Soc., Chem. Commun.* **1972**, 1339−1340. (b) Bowen, D. H.; Green, M.; Grove, D. M.; Moss, J. R.; Stone, F. G. A. Chemistry of the Metal Carbonyls. Part LXIX. Synthesis and Reactions of Complexes of Manganese Containing the Substituted and Unsubstituted 2,5-Dioxacyclopentylidene Ligand. *J. Chem. Soc., Dalton Trans.* **1974**, 1189−1194. (c) Daub, J.; Kappler, J. Thionocarbonat-Komplexe mit Übergangsmetallen der Gruppe VIB. Synthese von Eisentetracarbonyl-Carben-Complexen. *J. Organomet. Chem.* **1974**, *80*, C5−C8. (d) Pfiz, R.; Daub, J. Synthese und Struktur eines Benzodioxol-2-yliden-Eisen-Komplexes. *J. Organomet. Chem.* **1978**, *152*, C32−C34. (e) Le Bozec, H.; Gorgues, A.; Dixneuf, P. H. Novel Route to Iron-Carbene Derivatives via Addition of Alkynes to Carbon Disulfide-Iron Complexes. Rearrangement of 91,3-Dithiol-2-ylidene)iron Complexes into Heterometallacycles. *Inorg. Chem.* **1981**, *20*, 2486−2489. (f) Daub, J.; Endress, G.; Erhardt, U.; Jogun, K. H.; Kappler, J.; Laumer, A.; Pfiz, R.; Stezowski, J. J. Desulfurierungsreaktionen mit Eisencarbonyl-Verbindungen: Carbonyl(dioxolanyliden)-eisen-Komplexe aus Thionocarbonaten. *Chem. Ber.* **1982**, *115*, 1787−1809.

https://dx.doi.org/10.1021/acs.organomet.0c00066
Organometallics 2020, 39, 1762−1771

(g) Motschi, H.; Angelici, R. J. Synthesis of Cyclic Aminooxo- and Dioxocarbenes from Carbonyl Ligands in Complexes of Iron and Manganese. *Organometallics* **1982**, *1*, 343−349. (h) Singh, M. M.; Angelici, R. J. Dioxy Carbene Complexes from Reactions of $Fe(CO)_5$, $Mn(CO)_{10}$, $Re_2(CO)_{10}$ and $Ru(CO)_{12}$ with Oxirane. *Inorg. Chim. Acta* **1985**, *100*, 57−63. (i) Michelin, R. A.; Facchin, G.; Ros, R. Preparation of New Hydridoplatinum(II) Carbene Derivatives from Hydridotrifluoromethyl Complexes. *J. Organomet. Chem.* **1985**, *279*, C25−C28. (i) Miessler, G. L.; Kim, S.; Jacobson, R. A.; Angelici, R. J. Synthesis, Reactions, and Structures of Dioxycarbene Complexes of Rhenium. *Inorg. Chem.* **1987**, *26*, 1690−1695. (j) Wang, S.-J.; Miller, L. L.; Jacobson, R. A.; Angelici, R. J. Synthesis, Structure, and Catalytic Reactions of Dioxycarbene Complexes of Iron and Osmium. *Inorg. Chim. Acta* **1988**, *145*, 129−137. (k) Andrews, M. A.; Myles, W. L. Ketone-like Derivatization Reactions of Metal Carbonyls. Attempts to Measure the Equilibrium Constant for Ketalization of a Carbonyl Ligand in $[R(CO)_6]^+$ by Ethylene Glycol. *Inorg. Chem.* **1988**, *27*, 1118−1120. (l) Michelin, R. A.; Ros, R.; Guadalupi, G.; Bombieri, G.; Benetollo, F.; Chapuis, G. Electrophilic Cleavage of Carbon-Fluorine Bonds in Hydrido Trifluoromethyl Complexes of Platinum(II) by Proton Acids. Synthesis of Hydrido Carbene and Hydrido Carbonyl Derivatives and X-ray Structures of trans-$PtH(CF_3)(PPh_3)^2$ (180 K) and trans-$[PtH[cyclic](COCH_2CH_2O)(PPh_3)_2]BF_4$ (298 K). *Inorg. Chem.* **1989**, *28*, 840−846. (m) Glavee, G. N.; Su, Y.; Jacobson, R. A.; Angelici, R. Reactions of $CpFe(CO)_2(=[cyclic](COCH_2CH_2O))^+$, $CpFe(CO)_2[=C(SMe)_2]^+$ and Related Carbene Complexes with Reducing Agents and Nucleophiles. The Structure of $\{CpFe(CO)_2[=C(SMe)_2]\}PF_6$. *Inorg. Chim. Acta* **1989**, *157*, 73−84. (n) Miessler, G. L.; Kim, S.; Jacobson, R. A.; Angelici, R. J. Synthesis, Reactions, and Structures of Dioxycarbene Complexes of Rhenium. *Inorg. Chem.* **1987**, *26*, 1690−1695.

(14) (a) Le Bozec, H.; Gorgues, A.; Dixneuf, P. H. Novel Route to Iron-Carbene Complexes via η^2-CS_2 Derivatives. 1,3-Dithiolium Species as Precursors for Dithiolene-Iron Complexes and Tetrathiafulvalenes. *J. Am. Chem. Soc.* **1978**, *100*, 3946−3947. (b) Le Marouille, J. Y.; Lelay, C.; Benoit, A.; Grandjean, D.; Touchard, D.; Le Bozec, H.; Dixneuf, P. Sulfur-Containing Carbene-Metal Compounds: General Route from Carbon Disulfide Manganese Complexes; X-ray Structure of 1,3-Dithiol-2-ylidenemanganese(I) Derivative. *J. Organomet. Chem.* **1980**, *191*, 133−142. (c) Le Bozec, H.; Gorgues, A.; Dixneuf, P. H. Novel Route to Iron-Carbene Derivatives via Addition of Alkynes to Carbon Disulfide-Iron Complexes. Rearrangement of 91,3-Dthiol-2-ylidene)iron Complexes into Heterometallacycles. *Inorg. Chem.* **1981**, *20*, 2486−2489. (d) Singh, M. M.; Angelici, R. J. Expansion of Three-Membered Heterocycles to Five-Membered Cyclic Carbenes—Novel Reactions of Aziridine, Oxirane, and Thiirane with CO and CS Ligands in Iron, Ruthenium, and Manganese Complexes. *Angew. Chem., Int. Ed. Engl.* **1983**, *22*, 163−164; *Angew. Chem.* **1983**, *95*, 160. (e) Singh, M. M.; Angelici, R. J. Reactions of Aziridine, Oxirane and Thiirane with Carbonyl and Thiocarbonyl Ligands in Complexes of Iron, Manganese, and Ruthenium: Syntheses of Cyclic Carbene Compounds. *Inorg. Chem.* **1984**, *23*, 2691−2698. (f) Singh, M. M.; Angelici, R. J. Reactions of Aziridine and Oxirane with Manganese and Rhenium Carbonyl Complexes. Syntheses of Neutral 5-Membered Cyclic Aminooxy and Dioxycarbene Compounds. *Inorg. Chem.* **1984**, *23*, 2699−2705.

(15) (a) Liske, A.; Verlinden, K.; Buhl, H.; Schaper, K.; Ganter, C. Determining the π-Acceptor Properties of N-Heterocyclic Carbenes by Measuring the ^{77}Se NMR Chemical Shifts of Their Selenium Adducts. *Organometallics* **2013**, *32*, 5269−5272. (b) Nelson, D. J.; Collado, A.; Manzini, S.; Meiries, S.; Slawin, A. M. Z.; Cordes, D. B.; Nolan, S. P. Methoxy-Functionalized N-Heterocyclic Carbenes. *Organometallics* **2014**, *33*, 2048−2058. (c) Nelson, D. J.; Nahra, F.; Patrick, S. R.; Cordes, D. B.; Slawin, A. M. Z.; Nolan, S. P. Exploring the Coordination of Cyclic Selenoureas to Gold(I). *Organometallics* **2014**, *33*, 3640−3645. (d) Vummaleti, S. V. C.; Nelson, D. J.; Poater, A.; Gómez-Suárez, A.; Cordes, D. B.; Slawin, A. M. Z.; Nolan, S. P.; Cavallo, L. What can NMR Spectroscopy of Selenoureas and Phosphinidenes Teach Us About the π-Accepting Abilities of N-Heterocyclic Carbenes? *Chem. Sci.* **2015**, *6*, 1895−1904.

(16) For syntheses via olefin dissociation, see: (a) Cardin, D. J.; Cetinkaya, B.; Lappert, M. F. Transition metal-carbene complexes. *Chem. Rev.* **1972**, *72*, 545−574. (b) Cardin, D. J.; Cetinkaya, B.; Lappert, M. F.; Manojlović-Muir, L.; Muir, K. W. An electron-rich olefin as a source of coordinated carbene; synthesis of trans-$PtCl_2[C(NPhCH_2)_2]PEt_3$. *J. Chem. Soc. D* **1971**, *0*, 400−401 For deprotonation and transmetallation routes see ref 1c. and references therein.

(17) Tanaka, K.; Yoshida, K.; Ishida, T.; Kobayashi, A.; Nogami, T. First TOF Donors: Synthesis and Characterization of Dibenzo- and Dinaphthotetraoxafulvalenes. *Adv. Mater.* **2000**, *12*, 661−664.

(18) Due to decomposition of dibenzodithiolium tetrafluoroborate in the presence of $[IrCl_2(cod)]$, accessing the desired SHC complex via deprotonation also failed.

(19) Gülcemal, S.; Gökçe, A. G.; Çetinkaya, B. Iridium(I) N-Heterocyclic Carbene Complexes of Benzimidazol-2-ylidene: Effect of Electron Donating Groups on the Catalytic Transfer Hydrogenation Reaction. *Dalton Trans.* **2013**, *42*, 7305−7311.

(20) Ehlers, A. W.; Ruiz-Morales, Y.; Baerends, E. J.; Ziegler, T. Dissociation Energies, Vibrational Frequencies, and ^{13}C NMR Chemical Shifts of the 18-Electron Species $[M(CO)_6]^n$ (M = Hf-Ir, Mo, Tc, Ru, Cr, Mn, Fe). A Density Functional Study. *Inorg. Chem.* **1997**, *36*, 5031−5036.

(21) Scherowsky, G.; Weiland, J. Bildung und Reaktionen von 2-Carbena-1,3-benzodithiolen; Umsetzungen von 1,3-Benzodithioliumsalzen. *Justus Liebigs Ann. Chem.* **1974**, *1974*, 403−411.

(22) Tapu, D.; Dixon, D. A.; Roe, C. ^{13}C NMR Spectroscopy of "Arduengo-type" Carbenes and Their Derivatives. *Chem. Rev.* **2009**, *109*, 3385−3407.

(23) Crystallographic data for $\mathbf{3^N}$ in a different space group were reported by: Meredith, J. M.; Robinson, R.; Goldberg, K. I.; Kaminsky, W.; Heinekey, D. M. C-H Bond Activation by Cationic Iridium(III) NHC Complexes: A Combined Experimental and Computational Study. *Organometallics* **2012**, *31*, 1879−1887.

(24) (a) Niehues, M.; Erker, G.; Kehr, G.; Schwab, P.; Fröhlich, R.; Blacque, O.; Berke, H. Synthesis and Structural Features of Arduengo Carbene Complexes of Group 4 Metallocene Cations. *Organometallics* **2002**, *21*, 2905−2911. (b) Aktas, H.; Slootweg, J. C.; Schakel, M.; Ehlers, A. W.; Lutz, M.; Spek, A. L.; Lammertsma, K. N-Heterocyclic Carbene-Functionalized Ruthenium Phosphinidenes: What a Difference a Twist Makes. *J. Am. Chem. Soc.* **2009**, *131*, 6666−6667.

(25) See also: Schilling, B. E. R.; Hoffmann, R.; Lichtenberger, D. L. $CpM(CO)_2$(ligand) (Cp = Cyclopentadienyl, M = Metal) Complexes. *J. Am. Chem. Soc.* **1979**, *101*, 585−591.

(26) (a) Tolman, C. A. Steric Effects of Phosphorus Ligands in Organometallic Chemistry and Homogeneous Catalysis. *Chem. Rev.* **1977**, *77*, 313−348. (b) Kelly III, R. A.; Clavier, H.; Giudice, S.; Scott, N. M.; Stevens, E. D.; Bordner, J.; Samardjiev, I.; Hoff, C. D.; Cavallo, L.; Nolan, S. P. Determination of N-Heterocyclic Carbene (NHC) Steric and Electronic Parameters using the $[(NHC)Ir(CO)_2Cl]$ System. *Organometallics* **2008**, *27*, 202−210. (c) Wolf, S.; Plenio, H. Synthesis of (NHC)Rh(cod)Cl and (NHC)RhCl(CO)2 Complexes - Translation of the Rh- into the Ir-scale for the Electronic Properties of NHC Ligands. *J. Organomet. Chem.* **2009**, *694*, 1487−1492.

(27) Beck, G.; Lappert, M. F.; Hitchcock, P. B. Synthesis of the Sterically Hindered Complexes $[M(CO)_5(CNBR_2)]$[R = CH(SiMe3)2; M = Cr, Mo, or W]. Crystal Structure of $[Cr(CO)_5(CNBR_2)]$. *J. Organomet. Chem.* **1994**, *468*, 143−148.

(28) (a) Schönherr, H.-J.; Wanzlick, H.-W. Chemie Nucleophiler Carbene, XX HX-Abspaltung aus 1.3-Diphenylimidazoliumsalzen. Quecksilbersalz Carben Komplexe. *Chem. Ber.* **1970**, *103*, 1037−1046. (b) Guerret, O.; Solé, S.; Gornitzka, H.; Teichert, M.; Trinquier, G.; Bertrand, G. 1,2,4-Triazole-3,5-diylidene: A Building Block for Organometallic Polymer Synthesis. *J. Am. Chem. Soc.* **1997**, *119*, 6668−6669. (c) Guerret, O.; Solé, S.; Gornitzka, H.; Trinquier, G.; Bertrand, G. 1,2,4-Triazolium-5-ylidene and 1,2,4-Triazol-3,5-

https://dx.doi.org/10.1021/acs.organomet.0c00066
Organometallics 2020, 39, 1762−1771

diylidene as New Ligands for Transition Metals. *J. Organomet. Chem.* **2000**, *600*, 112−117.
(29) A CCDC database search revealed that C−Ag bond distances of structurally characterized linear bis(NHC) Ag complexes span from about 2.017 to 2.161 Å.
(30) (a) Wang, H. M. J.; Lin, I. J. B. Facile Synthesis of Silver(I)-Carbene Complexes. Useful Carbene Transfer Agents. *Organometallics* **1998**, *17*, 972−975. (b) Garrison, J. C.; Youngs, W. J. Ag(I) N-Heterocyclic Carbene Complexes: Synthesis, Structure, and Application. *Chem. Rev.* **2005**, *105*, 3978−4008.
(31) (a) Boehme, C.; Frenking, G. N-Heterocyclic Carbene, Silylene, and Germylene Complexes of MCl (M = Cu, Ag, Au). A Theoretical Study. *Organometallics* **1998**, *17*, 5801−5809. (b) Lin, J. C. Y.; Huang, R. T. W.; Lee, C. S.; Bhattacharyya, A.; Hwang, W. S.; Lin, I. J. B. Coinage Metal-N-Heterocyclic Carbene Complexes. *Chem. Rev.* **2009**, *109*, 3561−3598. (c) Batiste, L.; Chen, P. Coinage-Metal Mediated Ring Opening of cis-1,2-Dimethoxycyclopropane: Trends from the Gold, Copper, and Silver Fischer Carbene Bond Strength. *J. Am. Chem. Soc.* **2014**, *136*, 9296−9307.
(32) Nemcsok, D.; Wichmann, K.; Frenking, G. The Significance of π Interactions in Group 11 Complexes with N-Heterocyclic Carbenes. *Organometallics* **2004**, *23*, 3640−3646.
(33) Jerabek, P.; Roesky, H. W.; Bertrand, G.; Frenking, G. Coinage Metals Binding as Main Group Elements: Structure and Bonding of the Carbene Complexes $[TM(cAAC)_2]$ and $[TM(cAAC)_2]^+$ (TM = Cu, Ag, Au). *J. Am. Chem. Soc.* **2014**, *136*, 17123−17135.
(34) Landis, C. R.; Hughes, R. P.; Weinhold, F. Bonding Analysis of $TM(cAAC)_2$ (TM = Cu, Ag, and Au) and the Importance of Reference State. *Organometallics* **2015**, *34*, 3442−3449.
(35) Fulmer, G. R.; Miller, A. J. M.; Sherden, N. H.; Gottlieb, H. E.; Nudelman, A.; Stoltz, B. M.; Bercaw, J. E.; Goldberg, K. I. NMR Chemical Shifts of Trace Impurities: Common Laboratory Solvents, Organics, and Gases in Deuterated Solvents Relevant to the Organometallic Chemist. *Organometallics* **2010**, *29*, 2176−2179.
(36) Ball, R. G.; Graham, W. A. G.; Heinekey, D. M.; Hoyano, J. K.; McMaster, A. D.; Mattson, B. M.; Michel, S. T. Synthesis and Structure of Dicarbonylbis(η-pentamethylcyclopentadienyl)diiridium. *Inorg. Chem.* **1990**, *29*, 2023−2025.
(37) Çetinkaya, E.; Hitchcock, P. B.; Küçükbay, H.; Lappert, M. F.; Al-Juaid, S. Carbene complexes: XXIV. Preparation and Characterization of Two Enetetramine-derived Carbenerhodium(I) Chloride Complexes $RhCl(L^R)_3$ and $[RhCl(COD)L^R]$ (L^R = dCN(Me)Cu-(CH_4CNMe-*o*) and the Preparation and X-ray Structures of the Enetetramine L_2^R and its Salt $[L_2^R][BF_4]_2$. *J. Organomet. Chem.* **1994**, *481*, 89−95.
(38) (a) Liske, A.; Verlinden, K.; Buhl, H.; Schaper, K.; Ganter, C. Determining the π-Acceptor Properties of N-Heterocyclic Carbenes by Measuring the ^{77}Se NMR Chemical Shifts of Their Selenium Adducts. *Organometallics* **2013**, *32*, 5269−5272. (b) Engl, P. S.; Senn, R.; Otth, E.; Togni, A. Synthesis and Characterization of N-Trifluoromethyl N-Heterocyclic Carbene Ligands and Their Complexes. *Organometallics* **2015**, *34*, 1384−1395.
(39) Nakayama, J.; Sugiura, H.; Hoshino, M. Reaction of 1,3-Benzodithiol-2-ylidenes with Elemental Sulfur and Selenium: a Convenient Preparation of 2-Thioxo- and 2-Selenoxo-1,3-benzodithioles. *Tetrahedron Lett.* **1983**, *24*, 2585−2588.
(40) The common procedure for the synthesis of Ag carbene complexes using silver oxide in the presence of a hydroxide base and the carbene precursor salt failed. Instead, only the carbene dimerization product DBTTF was observed. The synthesis of benzodithiolium chloride, which would have allowed the exclusive use of Ag_2O (and thus circumvention of the use of a hydroxide base), was also not successful.
(41) Becke, A. D. Density-functional thermochemistry. III. The role of exact exchange. *J. Chem. Phys.* **1993**, *98*, 5648−5652.
(42) Frisch, M. J.; Trucks, G. W.; Schlegel, H. B.; Scuseria, G. E.; Robb, M. A.; Cheeseman, J. R.; Scalmani, G.; Barone, V.; Mennucci, B.; Petersson, G. A.; et al., *Gaussian 09, Rev. A.1*; Gaussian, Inc.: Wallingford, CT, USA, 2009.
(43) (a) *ADF2014*; SCM, Theoretical Chemistry, Vrije Universiteit: Amsterdam, The Netherlands; http://www.scm.com. (b) te Velde, G.; Bickelhaupt, F. M.; Baerends, E. J.; Fonseca Guerra, C.; van Gisbergen, S. J. A.; Snijders, J. G.; Ziegler, T. *J. Comput. Chem.* **2001**, *22*, 931−967. (c) Fonseca Guerra, C.; Snijders, J. G.; te Velde, G.; Baerends, E. J. Towards an order- N DFT method. *Theor. Chem. Acc.* **1998**, *99*, 391−403.
(44) Vosko, S. H.; Wilk, L.; Nusair, M. Accurate Spin-Dependent Electron Liquid Correlation Energies for Local Spin Density Calculations: a Critical Analysis. *Can. J. Phys.* **1980**, *58*, 1200−1211.
(45) Becke, A. D. Density-Functional Exchange-Energy Approximation with Correct Asymptotic Behavior. *Phys. Rev. A: At., Mol., Opt. Phys.* **1988**, *38*, 3098−3100.
(46) Perdew, J. P. Density-Functional Approximation for the Correlation Energy of the Inhomogeneous Electron Gas. *Phys. Rev. B: Condens. Matter Mater. Phys.* **1986**, *33*, 8822−8824.
(47) Grimme, S.; Ehrlich, S.; Goerigk, L. Effect of the Damping Function in Dispersion Corrected Density Functional Theory. *J. Comput. Chem.* **2011**, *32*, 1456−1465.
(48) (a) Versluis, L.; Ziegler, T. The Determination of Molecular Structures by Density Functional Theory. The Evaluation of Analytical Energy Gradients by Numerical Integration. *J. Chem. Phys.* **1988**, *88*, 322−328. (b) Fan, L.; Versluis, L.; Ziegler, T.; Baerends, E. J.; Ravenek, W. Calculation of Harmonic Frequencies and Harmonic Force Fields by the Hartree-Fock-Slater Method. *Int. J. Quantum Chem.* **1988**, *34*, 173−181.
(49) van Lenthe, E.; Ehlers, A. W.; Baerends, E. Geometry Optimizations in the Zero Order Regular Approximation for Relativistic Effects. J. *J. Chem. Phys.* **1999**, *110*, 8943−8953.
(50) (a) Morokuma, K. Why Do Molecules Interact? The Origin of Electron Donor-Acceptor Complexes, Hydrogen Bonding and Proton Affinity. *Acc. Chem. Res.* **1977**, *10*, 294−300. (b) Ziegler, T.; Rauk, A. On the Calculation of Bonding Energies by the Hartree Fock Slater Method. *Theor. Chim. Acta* **1977**, *46*, 1−10. (c) Ziegler, T.; Rauk, A. CO, CS, N_2, PF_3, and $CNCH_3$ as δ donors and π Acceptors. A theoretical study by the Hartree-Fock-Slater transition-state method. *Inorg. Chem.* **1979**, *18*, 1755−1759.
(51) Sheldrick, G. M. A Short History of SHELX. *Acta Crystallogr., Sect. A: Found. Crystallogr.* **2008**, *64*, 112−122. (SHELXS-97)
(52) Sheldrick, G. M. Crystal Structure Refinement with SHELXL. *Acta Crystallogr., Sect. C: Struct. Chem.* **2015**, *C71*, 3−8. (SHEXL-2014)
(53) Krause, L.; Herbst-Irmer, R.; Sheldrick, G. M.; Stalke, G. M. Comparison of Silver and Molybdenum Microfocus X-ray Sources for Single-crystal Structure Determination. *J. Appl. Crystallogr.* **2015**, *48*, 3−10. (SADABS)

https://dx.doi.org/10.1021/acs.organomet.0c00066
Organometallics 2020, 39, 1762−1771